

Collective and single-particle excitations in coupled quantum wires in magnetic fields

J.-B. Xia

*Instituto de Física de São Carlos, Universidade de São Paulo, São Carlos, SP 13560-970, Brazil
and National Laboratory for Superlattices and Microstructures, Institute of Semiconductors, Chinese Academy of Sciences,
Beijing 100083, China*

G.-Q. Hai

Instituto de Física de São Carlos, Universidade de São Paulo, São Carlos, SP 13560-970, Brazil

(Received 13 March 2002; published 24 June 2002)

The full spectra of magnetoplasmons and single-particle excitations are obtained of coupled one-dimensional electron gases in parallel semiconductor quantum wires with tunneling. We show the effects of the interwire Coulomb interaction and the tunneling, as well as the magnetic-field-induced localization on the elementary excitations in symmetric and asymmetric coupled quantum wire structures. The interaction and resonance between the plasmon and the intersubband single-particle excitations are found in magnetic fields.

DOI: 10.1103/PhysRevB.65.245326

PACS number(s): 71.45.Gm, 72.15.Nj, 73.50.Mx

I. INTRODUCTION

In coupled quantum wires, the Coulomb interaction between one-dimensional electron gases leads to the so-called optical and acoustic plasmon modes.¹ Tunneling between the wires modifies these plasmon modes, especially the acoustic one.²⁻⁴ When an asymmetry is introduced between the two wires, a very weak nonresonant tunneling opens up gaps in the acoustic plasmon mode resulting from a resonance between the acoustic plasmon and single-particle excitations. A transverse magnetic field in such systems affects the tunneling strength and also the single-particle and collective excitations.^{5,6} In Refs. 5 and 6 the far-infrared absorption spectra due to the intersubband (transverse) magnetoplasmon modes are calculated with and without tunneling between the wires. In such a spectrum, only the plasmon excitations at long wavelength limit ($q \rightarrow 0$) contribute to the absorption. To observe the absorption peaks result from the so-called intersubband plasmon modes, a four-subband model was used in their calculations (two subbands originated from each wire). The enhancement due to interwire exchange interaction of the tunneling gap between the symmetric and antisymmetric states was included in the calculation in Ref. 5, and three peaks were found in the absorption spectrum. They were attributed to the intersubband optical and acoustic plasmon modes (from the lowest symmetric state to first excited symmetric and antisymmetric states, respectively). However, no information was given for the intersubband plasmon mode due to tunneling induced two lowest subbands (the lowest symmetric and antisymmetric states). In Ref. 6 the tunneling effect was considered only for the two higher subbands, and the calculation was performed in the small-magnetic-field limit. One intersubband magnetoplasmon absorption peak from the ground state (no tunneling effect) to the higher empty states were found. It was also shown that a small magnetic field could induce a Landau damping of this plasmon mode. However, a clear overall picture of the single-particle and magnetoplasmon excitations in the system of coupled quantum wires has not been obtained so far. A similar situation occurs for these excita-

tions in coupled quantum wells in a parallel magnetic field. Magnetoplasmons were studied in double quantum wells in a parallel magnetic field where the tunneling was included within only the lowest order of perturbation.⁷

The presence of a transverse magnetic field in coupled quantum wires leads to the motion of the electrons in the wire direction being coupled to that in the lateral direction. The single-electron wave function in the lateral direction depends on the wave vector k in the wire direction. If we proceed in the standard manner of linear-response theory to derive the dispersion relation of the magnetoplasmons, we would have to solve a secular equation with infinite dimensions according to the wave vector k . This leads to difficulties in the calculations even within the random-phase approximation (RPA). In this work, the magnetoplasmon dispersions are obtained by projecting the electron states of the coupled wires to a basis constructed by the states of corresponding single wires. We show the effects of the tunneling strength and the magnetic-field-induced localization on the plasmon modes in such systems. We find a strong interaction between the collective modes and the single-particle excitations induced by transverse magnetic fields and tunneling.

II. THEORETICAL FORMALISM

We consider two coupled parallel quantum wires in the xy plane subjected a transverse magnetic field \mathbf{B} in the z -direction. The quantum wires are of zero thickness in the z direction. The confinement potential $V(y)$ in the y direction forms two quantum wires parallel to each other in the x direction. It is taken as square well type of widths W_1 and W_2 and barrier height V_b . The potential barrier between the two wires is of width W_b . The numerical calculation is applied to GaAs/Al_{0.3}Ga_{0.7}As structures with $V_b = 228$ meV.

The plasmon modes in such a system in the absence of magnetic field were studied in our previous work.^{2,3} However, a magnetic field in the z direction strongly affects the

single-particle and collective excitations, as will be shown below. The single-electron Hamiltonian in the present system can be written as

$$H_e = \frac{1}{2m^*} \left[p_x^2 + p_y^2 + \left(\frac{eB}{c} \right)^2 \left(y - \frac{c\hbar k}{eB} \right)^2 \right] + V(y), \quad (1)$$

where k is the electron wavevector in the x direction, m^* the electron effective mass, and e the electron charge. The above equation indicates that the effect of an external magnetic field is equivalent to an additional parabolic potential in the y direction, whose origin depends on the wave vector k and the magnetic field B . The eigenenergy and wave function in the y direction are functions of k noted by $E_n(k)$ and $\psi_{n,k}(y)$. We consider symmetric and also asymmetric two coupled wires with tunneling. The asymmetry is introduced by the different wire widths $W_1 \neq W_2$ and the tunneling strength is controlled by the barrier thickness between the wires. For the considered structures the excited states are much higher than the ground states of the two coupled wires. We restrict ourselves to the case of two ground states $n=1$ and 2 . For two symmetric quantum wires, the wave functions $\psi_{n,k}(y)$ at $k=0$ are symmetric ($n=1$) and antisymmetric ($n=2$) functions of y . For nonzero k , the wave function $\psi_{1,k}(y)$ shifts to one wire, while $\psi_{2,k}(y)$ to the other.

The screened Coulomb potential within the RPA is determined by the following self-consistent equation,

$$V_{\alpha k, \beta k'}^{sc}(q, \omega) = V_{\alpha k, \beta k'}^C(q) + \sum_{\gamma k''} V_{\alpha k, \gamma k''}^C(q) \times \Pi_{\gamma k'', \beta k'}^{(0)}(q, \omega) V_{\gamma k'', \beta k'}^{sc}(q, \omega), \quad (2)$$

with the bare Coulomb potential

$$V_{\alpha k, \beta k'}^C(q) = \frac{2e^2}{\epsilon_0} \int dy \int dy' \psi_{nk}(y) \psi_{n'k-q}(y) \times K_0(q|y-y'|) \psi_{m'k'+q}(y') \psi_{mk'}(y') \quad (3)$$

and

$$\Pi_{\beta k}^{(0)}(q, \omega) = \frac{f[E_{m'}(k)] - f[E_m(k-q)]}{E_{m'}(k) - E_m(k-q) + \hbar(\omega + i0^+)}, \quad (4)$$

where the indices $\alpha = \{n, n'\}$, $\beta = \{m, m'\}$, and $\gamma = \{l, l'\}$ represent pairs of the quantum numbers, and $f(E)$ is the Fermi distribution function.

In principle, the dispersion relation of the collective excitations can be obtained by the secular equation of the screened Coulomb potential defined by Eq. (2). However, it depends not only on the indices α and β but also on the wave vectors k and k' leading to a dielectric matrix of infinite dimensions which is not ‘‘properly’’ convergent in that a truncated submatrix with a finite dimension. For a system with a parabolic confinement potential, such as a single parabolic quantum well (wire) in a parallel (transverse) magnetic field, this difficulty was overcome by expanding the k -dependent wave function as a series of harmonic function so that the dielectric function is projected in a finite

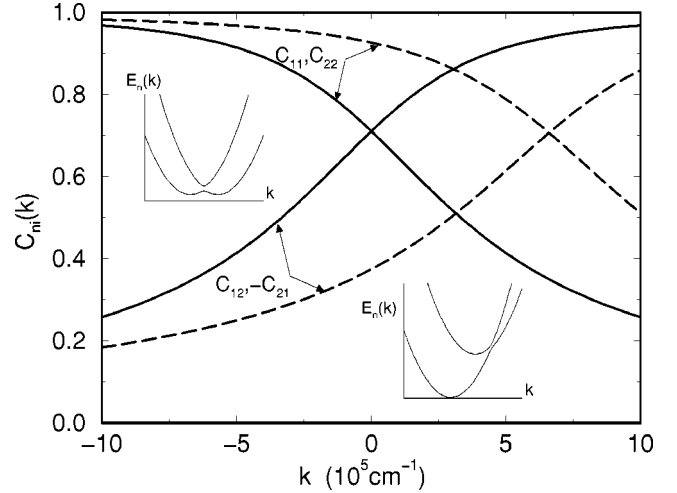


FIG. 1. The coefficients $C_{ni}(k)$ ($n, i=1$ and 2) at $B=1$ T for the symmetric (asymmetric) coupled quantum wires of $W_1=W_2=150$ Å ($W_1=150$ Å, $W_2=140$ Å) and $W_b=30$ Å are plotted by the solid (dashed) curves. The dispersion relations of a single-electron in the symmetric (asymmetric) structure are indicated in the left (low) inset.

submatrix.^{8,9} In this work, however, we choose another basis for our system of the coupled quantum wires. We consider the two quantum wires independently, and find the electron states in the single wires as a basis $\phi_i(y)$. The wave function $\psi_{nk}(y)$ of the coupled wires is expanded in this basis according to the k states. As will be shown below, we find it is enough to include only the ground states of the two single wires,

$$\psi_{nk}(y) = \sum_{i=1,2} C_{ni}(k) \phi_i(y), \quad (5)$$

where $i=1$ and 2 represent the ground states of the single wires W_1 and W_2 , respectively. The coefficients $C_{ni}(k)$ are shown as the solid curves in Fig. 1 for symmetric structures of $W_1=W_2=150$ Å and $W_b=30$ Å at $B=1$ T. The dispersion relations of the two subbands are schematically indicated in the inset on the left. At $k=0$, the expansion coefficients cross and their absolute values are $1/\sqrt{2}$, i.e., the electrons are distributed equally in the two wires. For large $|k|$, their absolute values approach to 1 or 0, indicating a magnetic-field-induced localization. The magnetic field pushes the electrons with $k<0$ in the $n=1$ ($n=2$) subband to the left wire W_1 (the right wire W_2). For those electrons with $k>0$, the magnetic field has the opposite effect. The expansion coefficients satisfy approximately the equation $\sum_{i=1,2} C_{ni}^2(k) = 1$ within a numeric error $<0.5\%$, indicating that the basis functions $\phi_1(y)$ and $\phi_2(y)$ are orthogonal and almost complete. For the asymmetric structure with $W_1=150$ Å, $W_2=140$ Å, and $W_b=30$ Å at $B=1$ T, the coefficients $C_{ni}(k)$ are given by the dashed curves. They cross at $k=6.6 \times 10^5$ cm⁻¹, where the anticrossing of the two subbands occurs as indicated by the lower inset in the figure.

With such an expansion, both the Coulomb potential $V_{\alpha k, \beta k'}^C(q)$ and the screened potential $V_{\alpha k, \beta k'}^{sc}(q, \omega)$ can be written in the form

$$V_{\alpha k, \beta k'} = \sum_{\xi, \eta} S_{\alpha k, \xi} S_{\beta k', \eta} v_{\xi, \eta}^C,$$

where $\xi = \{i, i'\}$ and $\eta = \{j, j'\}$ indicate pairs of the quantum numbers in our basis, and $S_{\alpha k, \xi} = C_{ni}(k-q)C_{n'i'}(k)$. As a consequence, Eq. (2) reduces to

$$\sum_{\eta'} \left(\delta_{\xi, \eta'} - \sum_{\xi'} v_{\xi, \xi'}^C(q) \Pi_{\xi', \eta'}(q, \omega) \right) v_{\eta', \eta}^{sc}(q, \omega) = v_{\xi, \eta}^C(q).$$

The dispersion relations of the magnetoplasmon excitations can be obtained by the equation

$$\text{Det} \left\{ \delta_{\xi, \eta} - \sum_{\xi'} v_{\xi, \xi'}^C(q) \Pi_{\xi', \eta}(q, \omega) \right\} = 0, \quad (6)$$

where

$$v_{\xi, \eta}^C(q) = \frac{2e^2}{\epsilon_0} \int dy \int dy' \phi_i(y) \phi_{i'}(y) \times K_0(q|y-y'|) \phi_j(y') \phi_{j'}(y') \quad (7)$$

and

$$\Pi_{\xi, \eta}(q, \omega) = \sum_{mm', k} C_{m'i}(k+q) C_{m'i'}(k) \times C_{mj}(k) C_{m'j'}(k+q) \Pi_{\beta k}^{(0)}(q, \omega). \quad (8)$$

III. NUMERICAL RESULTS AND DISCUSSIONS

Figure 2 shows the magnetoplasmon and the single-particle excitation (SPE) spectra of the two coupled symmetric quantum wires of $W_1 = W_2 = 150 \text{ \AA}$ with a total electron density $N_e = 10^6 \text{ cm}^{-1}$. The intrasubband (intersubband) SPE continua are indicated by the dark (light) shadow areas. Figures 2(a), 2(b), and 2(c) show structures of $W_b = 30 \text{ \AA}$ with different transverse magnetic fields $B = 0, 1, \text{ and } 2 \text{ T}$, respectively. In this structure, the tunneling-induced energy gap between the two subbands at zero magnetic field is $\Delta = 1.7 \text{ meV}$. Figure 2(d) is for the structure of $W_b = 70 \text{ \AA}$ at magnetic field $B = 1 \text{ T}$. In this case, $\Delta = 0.14 \text{ meV}$ at zero magnetic field indicating a much weaker tunneling.

The plasmon and SPE spectra at zero magnetic field as shown in Fig. 2(a) are similar to those of a single symmetric quantum wire with two occupied subbands. Two intrasubband (solid curves) and two intersubband plasmon modes (dash curves) are found, as discussed in Ref. 3. The symmetry of the system and the parabolicity of the subbands ensure that the intrasubband modes do not couple to the intersubband ones.

The transverse magnetic field pushes the electrons with $k < 0$ ($k > 0$) in the $n = 1$ and 2 ($n = 2$ and 1) subbands to the W_1 and W_2 wires, respectively, affecting the tunneling

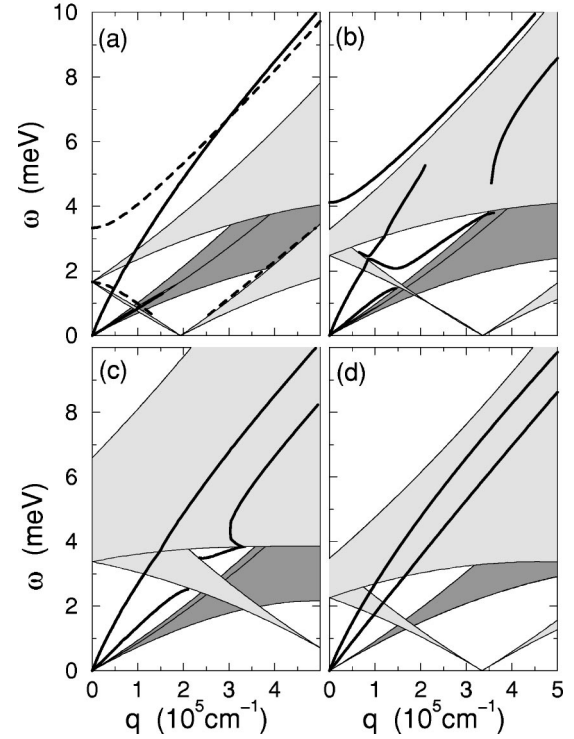


FIG. 2. The plasmon dispersions (thick curves), the intrasubband SPE (dark shadow), and the intersubband SPE (light shadow) continua in the symmetric coupled quantum wire structures of $W_1 = W_2 = 150 \text{ \AA}$ and $W_b = 30 \text{ \AA}$ at different magnetic fields (a) $B = 0$, (b) $B = 1 \text{ T}$ and (c) $B = 2 \text{ T}$. The results for the structure of $W_1 = W_2 = 150 \text{ \AA}$ and $W_b = 70 \text{ \AA}$ at $B = 1 \text{ T}$ are presented in (d). The total electron density $N_e = 10^6 \text{ cm}^{-1}$.

strength between the wires. In k space, the magnetic field leads to the two original parabolic subbands at $B = 0$ shifting to the opposite directions and the tunneling leads to an anti-crossing in the dispersion of the two subbands which is schematically shown in the left inset in Fig. 1. As a consequence, the intersubband SPE region is expanded, developing a band at $q = 0$. The magnetic field and tunneling-induced nonparabolicity in the subband dispersion results in interactions between the single-particle and the collective excitations. Such interactions are represented by the electron-electron scattering events during which only one of the electrons experiences an intersubband transition. When the momentum and energy transfer between the two electrons occurs in the intersubband SPE region, only one of the electrons creates an *intersubband* electron-hole pair, leading to charge tunneling between the wires due to the fact that the transverse magnetic field pushes the electron and the hole to opposite directions. On the other hand, the momentum and energy conservation guarantee the collective excitation due to such transitions, eliminating the so-called ‘‘Landau damping.’’ A resonance between the plasmon and the single-particle excitations occurs. Note that the interaction strength depends on the momentum transfer q . Figures 2(b) and 2(c) show the effects of these interactions on the magnetoplasmon modes at $B = 1$ and 2 T , respectively. At $B = 1 \text{ T}$ (corresponding to a cyclotron frequency $\omega_c = 1.65 \text{ meV}$ being close to $\Delta = 1.7 \text{ meV}$), tunneling is relatively strong, and so is the interaction between

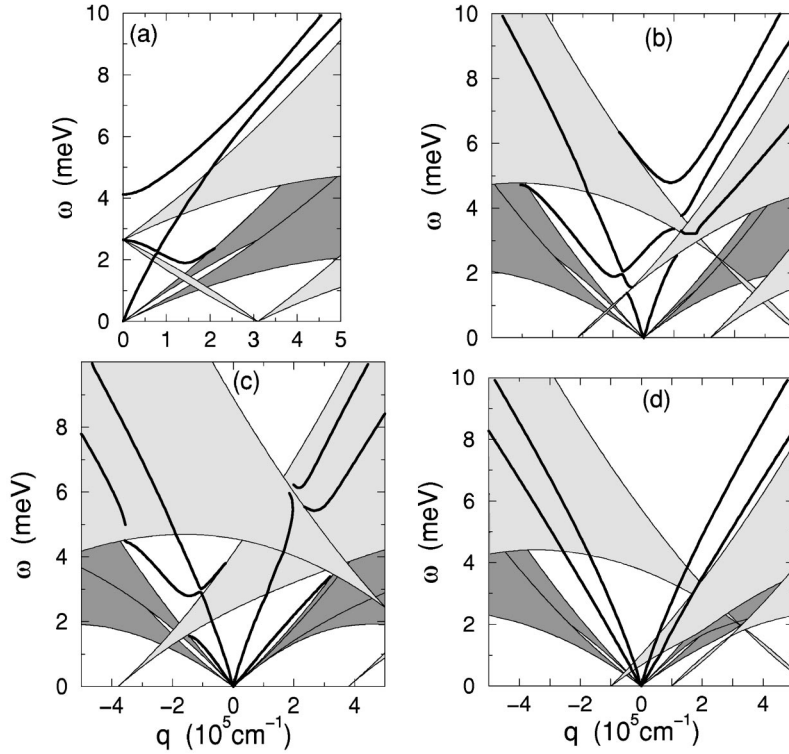


FIG. 3. The same as in Fig. 2, but now for the asymmetric structures with $W_1=150$ Å and $W_2=140$ Å.

the plasmon modes and the *intersubband* single-particle excitations. Figure 2(b) demonstrates this interaction, leading to (i) the high branch of the plasmon mode (above the intersubband SPE region and originally from the intersubband mode) keeping a distance from the SPE and (ii) a breaking at a certain energy of the plasmon mode in the *intersubband* SPE region. A larger transverse magnetic field leads to a strong localization of the electrons in each wire. The plasmon excitations restore their dispersion relation of two different modes, i.e., the optical and acoustic modes. Such a behavior is clearly seen in Figs. 2(c) and 2(d). In Fig. 2(c) the lower branch plasmon mode, i.e., the acoustic one, is still strongly modified due to its interaction with the intersubband SPE, showing a splitting when it approaches the SPE region at low frequencies. A magnetic field of 1 T for the structure with the larger barrier thickness of 70 Å is strong enough to suppress intersubband transitions completely, as indicated in Fig. 2(d), where the overlap of the electron wavefunctions of different subbands vanishes and so does the strength of the intersubband SPE.

Figure 3 shows the magnetoplasmon modes and the SPE spectra in two coupled asymmetric quantum wires. Comparing to Fig. 2(a), both the intersubband SPE and the plasmons in Fig. 3(a) shift to higher frequencies at small q because the energy gap between the two subbands increases to $E_2 - E_1 = 2.6$ meV by reducing the wire width W_2 to 140 Å. Although, at zero magnetic field, the asymmetry of the electron wave functions in real space leads to an anticrossing of the two high-frequency plasmon modes, as shown in Fig. 3(a), the electron states are symmetric in k space. However, a transverse magnetic field breaks the symmetry of the single-electron states in the k space, as indicated in the lower inset in Fig. 1. The electron gas has different Fermi wave vectors

for $k > 0$ and $k < 0$. Consequently, the plasmon dispersions and the SPE spectra are no longer symmetric functions of q . The asymmetric and nonparabolic subband structures leading to a strong coupling between the intersubband SPE and the plasmon modes are shown in Figs. 3(b) and 3(c). Figure 3(b) shows basically three plasmon modes in a V shape, but the electron-electron interaction results in an anticrossing and an even breaking up of these modes. The two branches with minima at $q = 0.95 \times 10^5$ and -0.97×10^5 cm⁻¹, respectively, are essentially intersubband modes. The one with $\omega = 0$ at $q = 0$ is an intrasubband (optical) plasmon mode. However, for $q > 1 \times 10^5$ cm⁻¹, the plasmon modes are strongly coupled to each other and also strongly interact with the intersubband SPE's. An anticrossing appears between the two higher branches. Moreover, the two lower branches break up at around $q = 1.2 \times 10^5$ cm⁻¹. At a larger magnetic field, the highest intersubband plasmon mode disappears, as shown in Fig. 3(c) but a lower-frequency intrasubband mode appears at small q which will eventually evolve into the so-called acoustic plasmon mode at large magnetic fields. Figure 3(d) shows the plasmon dispersions and the SPE spectra for the two coupled asymmetric quantum wires with $W_b = 70$ Å. In this case, the electrons in two different subbands are completely localized in different wires with a vanishing tunneling strength. An external magnetic field of 1 T almost does not affect the plasmon dispersion, which keeps its symmetry with respect to $q = 0$ as it is at zero magnetic field. Note that the intersubband SPE in this case is of a vanishing strength which has no effects on the plasmon modes.

IV. SUMMARY

In conclusion, the effects of a transverse magnetic field on single-particle and collective excitations are studied in

coupled quantum wires with tunneling. The magnetoplasmon spectra are obtained by an expansion of the electron states in a basis of the corresponding single quantum wires. The magnetic field modifies the electron subband structures and also the localization of the electron states, leading to a strong coupling between the collective and intersubband single-particle excitations. In two asymmetric quantum wires, the magnetic field results in the asymmetry of the plasmon and single-particle spectrum, increasing the flexibility to modulate the SPE and plasmon excitations, which may have some

applications in optical or magnetic switches. Our results also show that a larger transverse magnetic field leads to electron localization and completely suppresses the tunneling effects, leading to a recovery of the optical and acoustic plasmon modes.

ACKNOWLEDGMENTS

This work was supported by FAPESP and CNPq (Brazil) and the National Science Foundation (China) No.19874060.

-
- ¹T. Demel, D. Heitmann, P. Grambow, and K. Ploog, Phys. Rev. B **38**, 12 732 (1988); Phys. Rev. Lett. **66**, 2657 (1991); V. Shikin, T. Demel, and D. Heitmann, Phys. Rev. B **46**, 3971 (1992).
²G.Q. Hai and M.R.S. Tavares, Phys. Rev. B **61**, 1704 (2000).
³M.R.S. Tavares and G.Q. Hai, J. Phys.: Condens. Matter **13**, 6421 (2001).
⁴S. Das Sarma and E.H. Hwang, Phys. Rev. B **59**, 10 730 (1999).
⁵C. Steinebach, D. Heitmann, and V. Gudmundsson, Phys. Rev. B

- 56**, 6742 (1997); **58**, 13 944 (1998).
⁶T.V. Shahbazyan and S.E. Ulloa, Phys. Rev. B **54**, 16 749 (1996).
⁷G.R. Aizin and G. Gumbs, Phys. Rev. B **54**, 2049 (1996).
⁸L.H. Wang, Y. Zhu, F.A. Zeng, H.L. Zhao, and S.C. Feng, Phys. Rev. B **47**, 16326 (1993); L.H. Wang, F.A. Zeng, S.C. Feng, and Y. Zhu, *ibid.* **46**, 9804 (1992).
⁹L. Wendler and V.G. Grigoryan, Phys. Rev. B **54**, 8652 (1996); **49**, 13 607 (1994).